

3-(Hydroxyimino)imidazo[1,2-*a*]pyridin-2(3*H*)-ylidene)-1-arylethanones as new red heterocyclic dyes: Synthesis, spectral studies, quantum-chemical investigations, and antibacterial activities

Journal of Chemical Research

1–7

© The Author(s) 2019

Article reuse guidelines:

sagepub.com/journals-permissions

DOI: 10.1177/1747519819893060

journals.sagepub.com/home/chl



Nazanin Poormirzaei¹, Mehdi Pordel¹ , Elnaz Yaghoobi², Saeed Shojaee², Masoud Aminiyanfar¹ and Atoosa Gonabadi¹

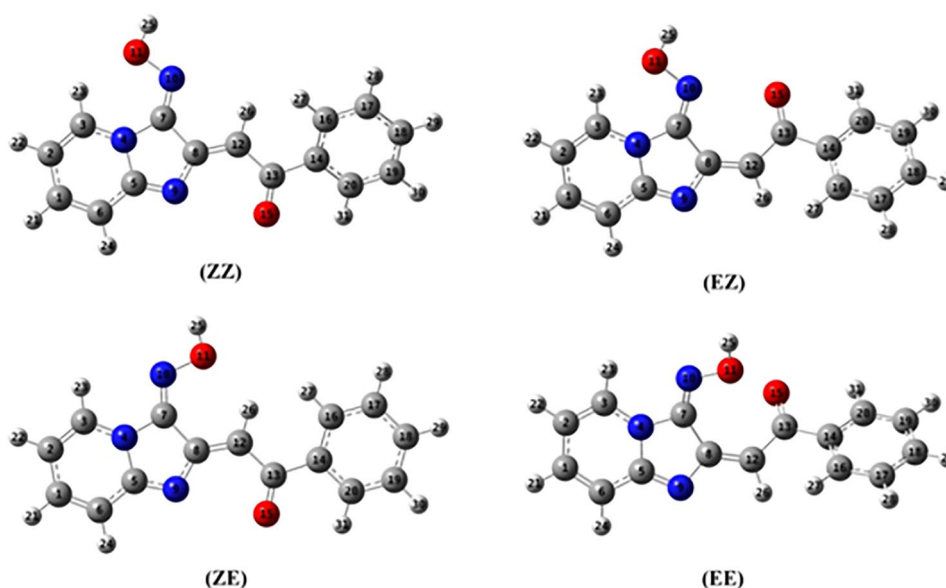
Abstract

The synthesis, optical properties, theoretical calculations, and antibacterial activities of a series of new red heterocyclic dyes derived from imidazo[1,2-*a*]pyridine are presented. 3-(Hydroxyimino)imidazo[1,2-*a*]pyridin-2(3*H*)-ylidene)-1-arylethanones are obtained from the reaction of 3-nitroimidazo[1,2-*a*]pyridine with substituted acetophenone derivatives in good yields (65%–72%). The structures are confirmed by spectral and analytical data, and the optical properties of the dyes are characterized by spectrophotometry. Density functional theory calculations are performed to provide the optimized geometries and relevant frontier orbitals. Calculated electronic absorption spectra are also obtained by the time-dependent density functional theory method. Moreover, the antibacterial activities (minimum inhibitory concentration) of the new dyes against Gram-positive and Gram-negative bacterial species are determined (minimum inhibitory concentration: 5–200 $\mu\text{g mL}^{-1}$).

Keywords

acetophenone, antibacterial activity, density functional theory, imidazo[1,2-*a*]pyridines, optical properties

Date received: 24 May 2019; accepted: 6 November 2019



¹Department of Chemistry, Islamic Azad University, Mashhad, Iran

²Department of Pharmaceutical Chemistry, Faculty of Pharmaceutical Chemistry, Pharmaceutical Science Branch, Islamic Azad University, Tehran, Iran

Corresponding author:

Mehdi Pordel, Department of Chemistry, Islamic Azad University, Mashhad Branch, Ostad Yusofei Street, Eamieh Boulevard, GasemAbad, Mashhad, Iran.

Email: mehdi.pordel58@mshdiau.ac.ir

Introduction

Heterocyclic dyes have wide applications in the dyestuff industries.^{1,2} The use of these dyes in the electronic industry, for example, as colorimetric sensors, nonlinear optical (NLO) devices, and liquid crystalline displays (LCDs), has been investigated, while their use as potential sensitizers for photodynamic therapy (PDT) has attracted much attention.³ In addition, they have been evaluated and employed as optoelectronic devices,⁴ photoconductors,⁵ sensitizers,⁶ biomedical probes,⁷ photo/catalysts,⁸ for solar-energy utilizations,⁹ and so on. Furthermore, heterocyclic dyes have been widely used in the preparation of disperse dyes with outstanding dischargeability on cellulose acetate.¹⁰

Imidazo[1,2-*a*]pyridines, as an important type of bicyclic nitrogen heterocycle, have been used for the production of dyes and some valuable drugs. They exhibit interesting biological properties such as antiviral,¹¹ anticancer,¹² anxiolytic,¹³ antimalarial,¹⁴ hypnotic,¹⁵ antiprotozoal,¹⁶ and anti-inflammatory¹⁷ activities, which has rendered this ring system an attractive target. Recently, imidazo[1,2-*a*]pyridine scaffolds became of interest as dye and fluorescent compounds.^{18–20} In some case, imidazo[1,2-*a*]pyridines with suitable functionalization can use as acid–base indicators.²¹

Based on these aspects and in continuation of our previous studies on the synthesis of new heterocyclic dyes,^{18–23} we have synthesized three new heterocyclic dyes in good yields from the reaction of 3-nitroimidazo[1,2-*a*]pyridine with substituted acetophenone derivatives in a basic medium. The optical properties, density functional theory (DFT)/time-dependent density functional theory (TD-DFT) calculations, and antibacterial activity of the dyes have also been examined.

Results and discussion

Synthesis and structures of the dyes **3a–c**

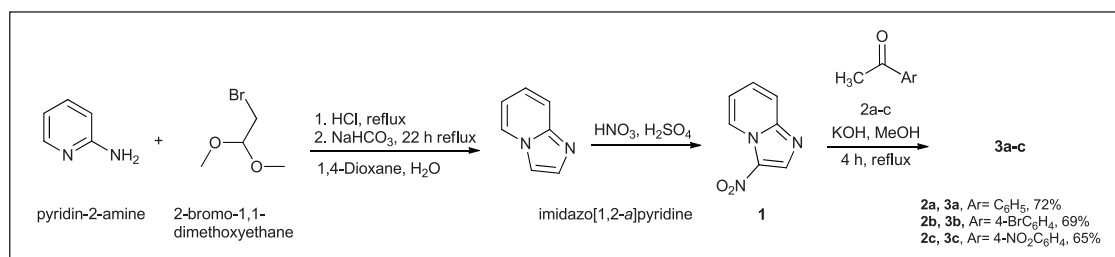
In order to the synthesis new dyes, the precursor 3-nitroimidazo[1,2-*a*]pyridine (**1**) was prepared in two steps. Initial reaction of pyridine-2-amine with 2-bromo-1,1-dimethoxyethane led to the formation of imidazo[1,2-*a*]pyridine.²⁴ Subsequent nitration of imidazo[1,2-*a*]pyridine in H₂SO₄ and HNO₃ produced 3-nitroimidazo[1,2-*a*]pyridine (**1**) according to a literature method.²⁵ The new 3-(hydroxyimino)imidazo[1,2-*a*]pyridin-2(3*H*)-ylidene)-1-arylethanones (**3a–c**) dyes were obtained in good yields from the condensation of 3-nitroimidazo[1,2-*a*]pyridine (**1**) and different acetophenone derivatives **2a–c** in basic MeOH solution via nucleophilic substitution²⁶ (Scheme 1).

The structural assignments of compounds **3a–c** were based on analytical and spectral data. In the ¹H NMR spectrum of **3a** the four signals at 8.87, 9.29, 10.04, and 10.08 ppm assignable to OH protons were attributed to four non-isolable isomers of **3a** (Figure 1). As depicted in Scheme 2, the most plausible reaction mechanism to explain the formation of the four isomers of **3a–c** involves attack of the anion derived from **2a–c** on compound **1** followed by dehydration of **A** and the formation of intermediate **B**. Finally, tautomerization of **B** in basic medium led to the formation of four isomers each of compounds **3a–c**. These isomeric relationships were not reported in similar reactions.^{18–23}

We made a several attempts to isolate the isomers by classical methods, but they could not be isolated from each other. This implies that the isomers can convert into each other. Recently, we performed DFT calculations by using the B3LYP hybrid functional and the 6-311++G(d,p) basis set to determine the most reasonable mechanism for the formation of 3*H*-imidazo[4,5-*a*]acridines.²⁷ According to these results, conversion of the isomers into each other can be facilitated by their tautomerization into intermediate **B**. In order to clarify the optimized geometry and energy of each isomer, DFT calculations were carried out at the B3LYP/6-311++G(d,p) level. The optimized geometries of the isomers **3a** can be found in Figure 2. Also, the sum of the electronic and zero-point energy and the relative energies (kJ mol⁻¹) of all the isomers in MeOH solution are reported in Table 1. As can be seen in Table 1, the energy difference between the four isomers is low and the isomer **3a³** is the most stable isomer in MeOH solution.

The data from the NOESY experiment on compound **3a** did not show a cross-peak between the OH protons and other protons in the isomers, and we are thus unable to assign the OH groups of the four isomers in DMSO-*d*₆ (not shown). However, the DFT-calculated chemical shifts of compounds **3a–c** can help identify the structures of the isomers. For example, the DFT-calculated chemical shifts of the isomers of **3a** show that the shift OH protons in **3a¹–a⁴** are 9.05, 9.33, 9.91, and 10.01 ppm, respectively, and therefore, in the ¹H NMR spectrum of **3a**, the signals at 8.87, 9.29, 10.04, and 10.08 ppm are assigned to the OH protons of **3a¹**, **3a²**, **3a³**, and **3a⁴**, respectively.

The percentage of isomers can be easily obtained from integrations. Similarly, the percentage of each isomer in compounds **3a–c** can be determined from the ¹H NMR spectra. The isomer ratios of each isomer in compounds **3a–c** can be obtained from the relative integrations of the OH group in the ¹H NMR spectra of compounds **3a–c**.



Scheme 1. Synthesis of new dyes **3a–c**.

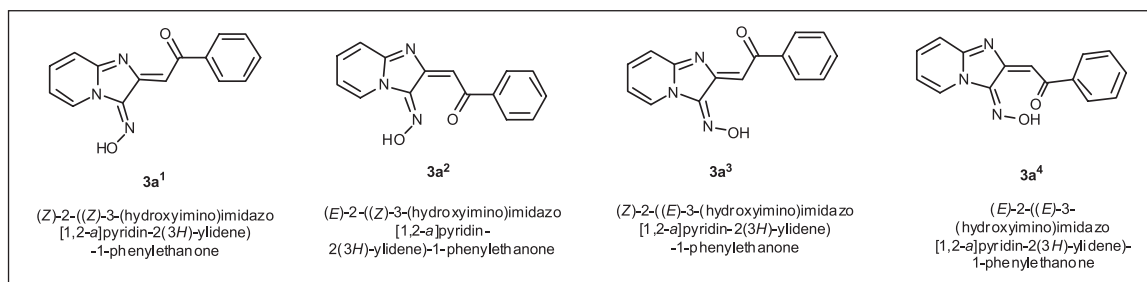
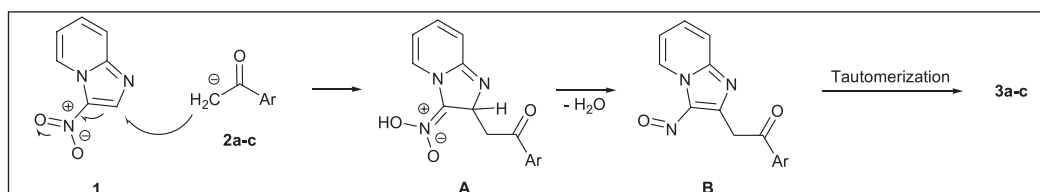


Figure 1. Structures of the isomers of 3a.



Scheme 2. A plausible reaction mechanism for the formation of 3a-c.

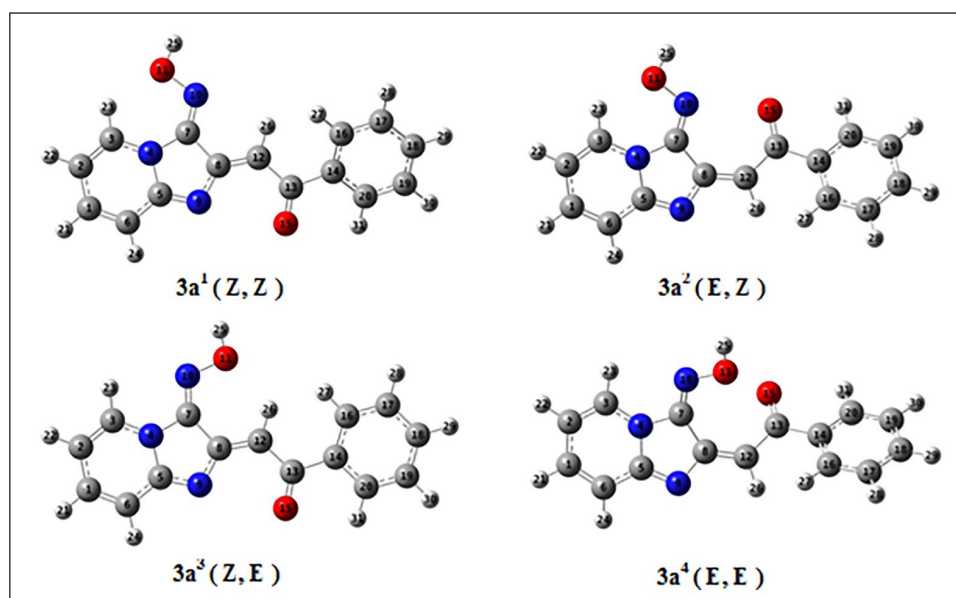


Figure 2. Optimized geometries of the isomers of 3a.

Table 2 shows the detailed results of each reaction, including the yields and isomer ratios in compounds 3a-c.

Optical properties

The new dyes 3a-c were deep red in color. The compounds were characterized by their UV-Vis spectra. Figure 3 shows the visible absorption spectra of dyes 3a-c in methanol solution (3×10^{-5} M). The characteristics of the absorption spectra of 3a-c in MeOH are presented in Table 3. The values of the extinction coefficient (ϵ) were calculated as the slope of the plot of absorbance versus concentration. The absorbance intensity and extinction coefficient (ϵ) of red dye 3c were the highest.

The absorption spectra of dyes 3a-c were measured in different solvents. As shown in Table 4, the absorption

Table 1. Energies (kJ mol⁻¹) of the isomers of 3a.

Isomer	E (pcm) ^a	ΔE (PCM) ^b
3a ¹	2344720.247	1.016
3a ²	2344707.889	13.274
3a ³	2344721.263	0
3a ⁴	2344705.942	15.321

PCM: Polarized Continuum Model.

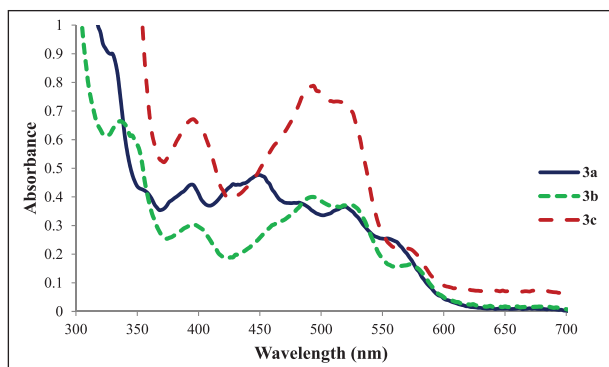
^aSum of the electronic and zero-point energies.

^bRelative energy to 3a³.

spectra of 3a-c in polar solvents undergo a red shift. Increasing the solvent polarity stabilizes the excited state molecule comparative to the ground-state molecule, with the observed red shift of the absorption maximum as the experimentally observed result (Table 3). For example, in the

Table 2. The detailed results of each reaction including the yields and percentage of isomers in compounds **3a–c**.

Entry	Compound	R	Yield %	Isomer 1 (Z, Z) (%)	Isomer 2 (E, Z) (%)	Isomer 3 (Z, E) %	Isomer 4 (E, E) (%)
1	3a	H	72	27.9	23.5	24	24.6
2	3b	Br	69	27.5	23.9	24.2	24.4
3	3c	NO ₂	65	28.2	23	23.4	25.4

**Figure 3.** Visible absorption spectra of dyes **3a–c** in methanol solution ($3 \times 10^{-5} \text{ mol L}^{-1}$).

absorption spectra of dye **3c**, λ_{abs} shifts from 425 to 495 nm as the solvent changes from *n*-hexane to DMSO (Table 4).

The color intensity of the dyes **3a–c** indicates efficient intramolecular charge transfer (ICT) states^{18–23} from the donor site (endocyclic N-4 and OH group) to the acceptor moiety (C=O group) (Scheme 3). To gain a deeper insight into the optical properties and the UV-Vis absorption spectra of the dyes, we performed DFT and TD-DFT calculations at the B3LYP/6-311++G(d,p) level and obtained HOMO and LUMO frontier orbitals and electronic spectra of isomers **3a¹–a⁴**.

The energy difference between the HOMO and LUMO frontier orbitals is one of the important characteristics of molecules, which has a determining role in such cases as electric properties, electronic spectra, and photochemical reactions. The HOMO and LUMO maps of **3a¹–a⁴** are shown in Figure 4. As can be seen, the HOMOs and LUMOs of **3a¹–a⁴** are totally localized on the OH (donor site) and C=O (acceptor site) groups. The separation energies between the HOMO and LUMO ($\Delta\varepsilon = \varepsilon_{\text{LUMO}} - \varepsilon_{\text{HOMO}}$) in isomers **3a¹–a⁴** are 2.77, 2.81, 2.79, and 2.88 eV, respectively.

The calculated electronic absorption spectra were also obtained by the time-dependent density functional theory (TD-DFT) method. The TD-DFT electronic spectra calculations on of **3a¹–a⁴** show two electronic transition bands. There is a relatively sharp peak at 347–353 nm (oscillator strength: 0.1041–0.2682), which can be attributed to $\pi-\pi^*$ transitions (donor endocyclic N-4 to the acceptor C=O group) (experimental value: 389 nm) and a relatively broad band at 505–520 nm with an oscillator strength of 0.2674–0.3492, which can be linked to $n-\pi^*$ transitions from the donor OH group to the acceptor C=O group, compared with the experimental values of 450–550 nm.

The calculated electronic absorption spectra of non-isolable isomers **3a¹–a⁴** are shown in Figure 5.

Antibacterial studies

The antibacterial activity of new dyes **3a–c** was tested against a panel of strains of Gram positive (*Staphylococcus aureus*, methicillin-resistant *S. aureus* (MRSA) clinical isolated and *Bacillus subtilis* (ATCC 6633)) and Gram negative (*Pseudomonas aeruginosa* (ATCC 27853) and *Escherichia coli*, (ATCC 25922)) bacterial species (Table 4) using the broth microdilution method as previously described.²⁸ Ampicillin, penicillin G, and sulfamethoxazole were used as references. The lowest concentration of the antibacterial agent that prevents growth of the test organism, as detected by lack of visual turbidity (matching the negative growth control), is designated the minimum inhibitory concentration (MIC). Experimental details of the tests can be found in our earlier study.^{29,30}

As shown in Table 4, compounds **3a–c** are effective against Gram-negative bacteria. Also, the results revealed that new dye **3c**, with an Ar=C₆H₄NO₂ group, displayed greater antibacterial activity against Gram-negative bacteria compared with the well-known antibacterial agents ampicillin and sulfamethoxazole (Table 4).

Conclusion

In conclusion, we have synthesized three new red dyes in good yields via nucleophilic substitution of the hydrogen of 3-nitroimidazo[1,2-*a*]pyridine with different acetophenone derivatives in basic methanol solution. The ¹H NMR spectra of the products revealed that the dyes exist as four non-isolable isomers. Although data from NOESY experiments did not allow assignment of the OH groups of the four isomers, the DFT-calculated chemical shifts of compounds **3a–c** helped to identify the structures of the isomers. The optical properties of the dyes were examined and the solvent effects on the absorption spectra of the dyes were studied. DFT and TD-DFT calculations of the dyes were performed to obtain HOMO and LUMO frontier orbitals and electronic spectra by using the B3LYP hybrid functional and the 6-311++G(d,p) basis set. Furthermore, the electronic spectra of the dyes were in relatively good agreement with visible absorption spectra. Moreover, results from the antimicrobial screening tests showed that these new compounds were effective against standard strains of Gram-negative growth inhibitors. This property, together with optical properties, offers an excellent opportunity for the study of the physiological functions of bacteria such as at single-cell level.³¹

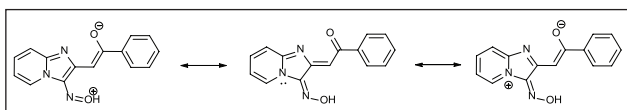
Further investigations into the scope and application of these new dyes are in progress and will be reported soon.

Table 3. Spectroscopic data for **3a–c** at 298 K showing dependence on the solvent.

Solvent	λ_{abs} (nm) ^a 3a	$\epsilon \times 10^{-3}$ (M ⁻¹ cm ⁻¹) ^b 3a	λ_{abs} (nm) ^a 3b	$\epsilon \times 10^{-3}$ (M ⁻¹ cm ⁻¹) ^b 3b	λ_{abs} (nm) ^a 3c	$\epsilon \times 10^{-3}$ (M ⁻¹ cm ⁻¹) ^b 3c
n-hexane	405	5.8	430	3.9	425	11.0
EtOAc	430	9.5	460	7.0	460	15.6
MeCN	440	14.5	478	10.8	480	22.0
DMF	445	15.0	485	11.0	490	22.5
DMSO	445	15.4	490	11.5	495	23.3
MeOH	449	17	498	13	494	25.7

^aWavelengths of maximum absorbance (λ_{max}).^bExtinction coefficients.**Table 4.** Antibacterial activity (MIC, $\mu\text{g mL}^{-1}$) of references and compounds **3a–c**.

Compound	S.a. (MRSA) ^a	B.s. (ATCC 6633) ^b	P.a. (ATCC 27853) ^c	E.c. (ATCC 25922) ^d
3a	>200	>200	25	20
3b	>200	>200	15	15
3c	>200	>200	10	5
Ampicillin	62	0.50	125	8
Penicillin G	60	8	–	–
Sulfamethoxazole	16	16	62	16

^a*Staphylococcus aureus* (methicillin-resistant *S. aureus*).^b*Bacillus subtilis*.^c*Pseudomonas aeruginosa*.^d*Escherichia coli*.**Scheme 3.** Some mesomeric structures of **3a**³.

Experimental

Materials

All reagents and solvents used in this work were purchased from Merck. The microorganisms *Bacillus subtilis* ATCC 6633, *Pseudomonas aeruginosa* ATCC 27853, and *Escherichia coli* ATCC 25922 were purchased from the Pasteur Institute of Iran and MRSA was isolated from different specimens which were referred to the Microbiological Laboratory of the Ghaem Hospital of the Medical University of Mashhad, Iran, and its methicillin resistance was tested according to the national committee for clinical laboratory standards (NCCLS) guidelines.³² All solvents were dried according to standard procedures. Compound **1** was synthesized according to a literature method.^{24,25}

Equipment

Absorption spectra were recorded on a Varian Cary 50-bio UV-Vis spectrophotometer. UV-Vis scans were recorded from 200 to 1000 nm. Melting points were measured on an Electro thermal type-9100 melting-point apparatus. The IR (as KBr disks) spectra were obtained on a Tensor 27 spectrometer and only noteworthy absorptions are listed. The ¹³C NMR (100 MHz), ¹H NMR (400 MHz) and NOESY

spectra were recorded on a Bruker Avance DRX-400 Fouriertransform spectrometer in DMSO-*d*₆. Chemical shifts are reported in parts per million downfield from tetramethylsilane (TMS) as the internal standard; coupling constants (*J*) are given in hertz. The mass spectra were recorded on a Varian Mat, CH-7 at 70 eV. Elemental analysis was performed on a Thermo Finnigan Flash EA microanalyzer. All measurements were carried out at room temperature.

Computational methods

The DFT calculations were performed with the Gaussian 98 software package³³ by using the B3LYP hybrid functional³⁴ and the 6-311++G (d,p) basis set. The geometries of the compounds were fully optimized in MeOH solution.

Here, one of self-consistent reaction field methods, the sophisticated Polarized Continuum Model (PCM)³⁵ was used for investigation of the solvent effects. The PCM calculations were performed in MeOH, and zero-point corrections were considered to obtain the energies. Based on the optimized geometries and using time-dependent density functional theory (TD-DFT)^{36–38} methods, the electronic spectra of the compounds were predicted.

The ¹H NMR chemical shifts of the compounds were predicted with respect to TMS. Here, the gauge-independent atomic orbital method (GIAO) was used for prediction of DFT nuclear shielding.³⁹

Synthesis of **3a–c** from **1** and **2a–c**

3-Nitroimidazo[1,2-*a*]pyridine (**1**) (3.26 g, 20 mmol) and substituted acetophenones **2a–c** (30 mmol) were added

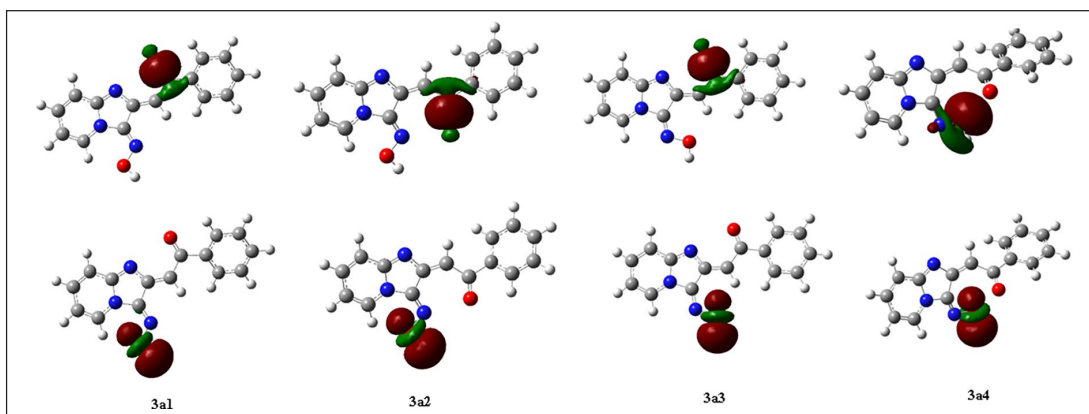


Figure 4. The HOMO (bottom) and LUMO (up) frontier orbitals of the dyes **3a1–a4**.

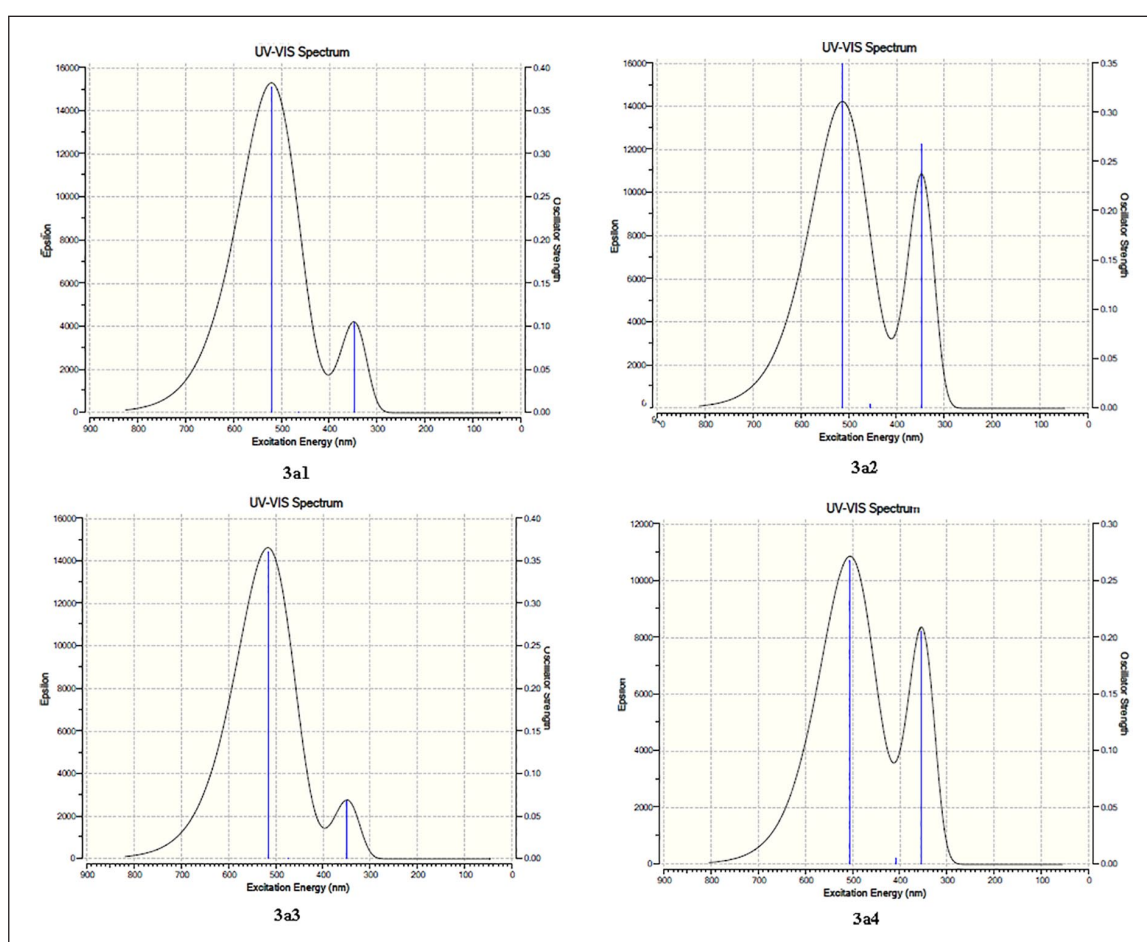


Figure 5. The calculated electronic absorption spectra of isomers **3a1–a4**.

with stirring to a solution of KOH (20 g, 357 mmol) in methanol (50 mL). The mixture was stirred at reflux for 4 h and then poured into water. After neutralization with dilute HCl solution, the precipitate was collected by filtration, washed with water, and then air on silica gel dried to give crude **3a–c**. Further purification was achieved by column chromatography on silica gel.

3-(Hydroxyimino)imidazo[1,2-*a*]pyridin-2(3*H*)-ylidene-1-phenylethanone (**3a**): Purified by silica gel column chromatography (CHCl₃-MeOH, 15:3) to give a

dark red powder, yield (72%), mp > 300 °C. IR (KBr): 1569 (m) (C=C), 1631 (s) (C=O), 3374 (m) (OH) cm⁻¹. ¹H NMR (DMSO-*d*₆): δ = 6.75 (1H, d, *J* = 6.7 Hz, pyridine H), 6.97 (1H, t, *J* = 7.1 Hz, pyridine H), 7.35–7.65 (6H, m, ArH), 7.71–7.84 (2H, m, ArH); 8.87 (br s, 27.9% of 1H, OH), 9.29 (br s, 23.5% of 1H, OH), 10.04 (br s, 24.0% of 1H, OH), 10.08 (br s, 24.6% of 1H, OH). ¹³C NMR (DMSO-*d*₆): δ = 102.9, 112.5, 122.5, 132.0, 133.3, 134.2, 136.7, 141.9, 147.3, 152.8, 159.8, 167.7, 192.5. MS (*m/z*): 265 (M⁺). Anal. Calcd for C₁₅H₁₁N₃O₂

(265.3): C, 67.92; H, 4.18; N, 15.84, Found: C, 68.12; H, 4.21; N, 15.65.

1-(4-Bromophenyl)-2-(3-(hydroxyimino)imidazo[1,2-a]pyridin-2(3H)-ylidene)ethanone (**3b**): Purified by a silica gel column chromatography (CHCl₃-MeOH, 18:4) to give a dark red powder, yield (69%), mp > 300 °C. IR (KBr): 1569 (m) (C=C), 1631 (s) (C=O), 3374 (m) (OH) cm⁻¹. ¹H NMR (DMSO-d₆): δ = 6.77 (1H, d, J = 6.7 Hz, pyridine H), 7.01 (1H, t, J = 7.1 Hz, pyridine H), 7.39 (1H, s, Alkene H), 7.55 (2H, d, J = 8.6 Hz, 4-bromophenyl H), 7.69–7.87 (4H, m, ArH); 8.96 (br s, 27.5% of 1H, OH), 9.33 (br s, 23.9% of 1H, OH), 10.09 (br s, 24.2% of 1H, OH), 10.12 (br s, 24.4% of 1H, OH). ¹³C NMR (DMSO-d₆): δ = 103.4, 113.4, 123.4, 128.3, 134.8, 135.1, 135.7, 141.6, 147.2, 152.8, 158.5, 166.8, 191.9. MS (m/z): 345 [M(⁸¹Br)]⁺, 343 [M(⁷⁹Br)]⁺. Anal. Calcd for C₁₅H₁₀N₃O₂Br (344.2): C, 52.35; H, 2.93; N, 12.21, Found: C, 52.17; H, 2.90; N, 12.55.

3-(Hydroxyimino)imidazo[1,2-a]pyridin-2(3H)-ylidene)-1-(4-nitrophenyl)ethanone (**3c**): Purified by silica gel column chromatography (CHCl₃-MeOH, 4:1) to give a dark red powder, yield (65%), mp > 300 °C. IR (KBr): 1335, 1575 (s) (NO₂), 1569 (m) (C=C), 1631 (s) (C=O), 3374 (m) (OH) cm⁻¹. ¹H NMR (DMSO-d₆): δ = 6.81 (1H, d, J = 6.7 Hz, pyridine H), 7.02 (1H, t, J = 7.1 Hz, pyridine H), 7.41 (1H, s, Alkene H), 7.73–7.85 (2H, m, ArH), 8.17 (2H, d, J = 8.7 Hz, 4-nitrophenyl H), 8.49 (2H, d, J = 8.7 Hz, 4-nitrophenyl H), 8.99 (br s, 28.2% of 1H, OH), 9.36 (br s, 23.0% of 1H, OH), 10.05 (br s, 23.4% of 1H, OH), 10.09 (br s, 25.4% of 1H, OH). ¹³C NMR (DMSO-d₆): δ = 103.6, 113.9, 122.2, 124.8, 134.3, 135.1, 135.9, 147.8, 152.3, 152.8, 158.5, 166.8, 191.7. MS (m/z): 310 (M⁺). Anal. Calcd for C₁₅H₁₀N₄O₄ (310.3): C, 58.07; H, 3.25; N, 18.06, Found: C, 57.85; H, 3.21; N, 17.90.

Declaration of conflicting interests

The author(s) declared no potential conflicts of interest with respect to the research, authorship, and/or publication of this article.

Funding

The author(s) disclosed receipt of the following financial support for the research, authorship, and/or publication of this article: We express our sincere gratitude to the Research Office, Mashhad Branch, Islamic Azad University, Mashhad, Iran, for financial support of this work.

ORCID iD

Mehdi Pordel  <https://orcid.org/0000-0003-3445-8792>

References

- Bhatti HS and Seshadri S. *Color technol* 2004; 120: 151.
- Shridhar AH, Keshavayya J and Hoskeri J. *Int J Pharm Pharm Sci* 2002; 4: 386.
- Faustino H, Brannigan CR, Reis LV, et al. *Almeida Dyes Pigm* 2009; 83: 88.
- Kalyanasundaram K and Grätzel M. *Coordination Chem Rev* 1998; 177: 347.
- Aihara S, Hirano Y, Tajima T, et al. *Appl Phys Lett* 2003; 82: 511.
- Shi J, Chai Z, Su J, et al. *Dyes Pigm* 2013; 98: 405.
- Te Velde E, Veerman T, Subramaniam V, et al. *Eur J Surg Oncology* 2010; 36: 6.
- Hsueh CL, Lu YW, Hung CC, et al. *Dyes Pigm* 2007; 75: 130.
- Polo AS, Itokazu MK and Iha NYM. *Coordination Chem Rev* 2004; 248: 1343.
- Maradiya HR. *J Saudi Chem Soc* 2010; 14: 77.
- Gudmundsson KS and Johns BA. *Org Letters* 2003; 5: 1369.
- Wu Z, Fraley ME, Bilodeau MT, et al. *Bioorg Med Chem Lett* 2004; 14: 909.
- Geronikaki A, Babaev E, Dearden J, et al. *Bioorg Med Chem* 2004; 12: 6559.
- Lima PC, Avery MA, Tekwani BL, et al. *Farmacology* 2002; 57: 825.
- Trapani G, Franco M, Ricciardi L, et al. *J Med Chem* 1997; 40: 3109.
- Ismail MA, Brun R, Wenzler T, et al. *J Med Chem* 2004; 47: 3658.
- Abe Y, Kayakiri H, Satoh S, et al. *J Med Chem* 1998; 41: 4053.
- Rahimizadeh M, Pordel M, Bakavoli M, et al. *Dyes Pigm* 2010; 86: 266.
- Baf MMF, Pordel M and Daghighi LR. *Tetrahedron Lett* 2014; 55: 6925.
- Rahimizadeh M, Pordel M, Ranaei M, et al. *J Heterocycl Chem* 2012; 49: 208.
- Razmara S, Pordel M and Ebrahimi M. *Chem Heterocyclic Comps* 2015; 51: 713.
- Poorhaji S, Pordel M and Ramezani S. *J Mol Struct* 2016; 1119: 151.
- Pordel M, Beyramabadi SA and Mohammadinejad A. *Dyes and Pigm* 2014; 102: 46.
- Roe AM. *J Chem Soc* 1963; 2195.
- Paolini JP and Robins RK. *J Org Chem* 1965; 30: 4085.
- Małkoza M and Wojciechowski K. *Chem Rev* 2004; 104: 2631.
- Zonozi F, Beyramabadi SA, Pordel M, et al. *Res Chem Intermed* 2017; 43: 1829.
- Tezer N and Karakus N. *J Mol Model* 2009; 15: 223.
- Pordel M, Ramezani S, Jajarmi M, et al. *Russ J Bioorg Chem* 2016; 42: 106.
- Pordel M, Abdollahi A and Razavi B. *Russ J Bioorg Chem* 2013; 39: 240.
- Sztaricskai F, Pintér G, Röth E, et al. *J Antibiot* 2007; 60: 529.
- Joux F and Lebaron P. *Microbes Infect* 2000; 2: 1523.
- Frisch M, Trucks G, Schlegel H, et al. Pittsburgh, PA, 1998.
- Lee C, Yang W and Parr RG. *Physical Rev B* 1988; 37: 785.
- Cammi R and Tomasi J. *J Comput Chem* 1995; 16: 1449.
- Bauer D and Ceccherini F. *Opt Express* 2001; 8: 377.
- Petersilka M, Gossmann U and Gross E. *Phys Rev Lett* 1996; 76: 1212.
- Bauernschmitt R and Ahlrichs R. *Chem Phys Lett* 1996; 256: 454.
- Wolinski K, Hinton JF and Pulay P. *J Am Chem Soc* 1990; 112: 8251.